Earth Surf. Dynam., 2, 295–308, 2014
www.earth-surf-dynam.net/2/295/2014/
doi:10.5194/esurf-2-295-2014

Earth Surface Dynamics
Open Access

Coastal vulnerability of a pinned, soft-cliff coastline – Part I: Assessing the natural sensitivity to wave climate

A. Barkwith[1], C. W. Thomas[1], P. W. Limber[2,*], M. A. Ellis[1], and A. B. Murray[2]

[1]British Geological Survey, Keyworth, Nottingham, NG12 5GG, UK
[2]Nicholas School of the Environment, Duke University, Durham, NC, USA
[*]now at: Dept. of Geological Sciences, University of Florida, Gainesville, FL, USA

Correspondence to: A. Barkwith (andr3@bgs.ac.uk)

Received: 23 September 2013 – Published in Earth Surf. Dynam. Discuss.: 19 November 2013
Revised: 7 April 2014 – Accepted: 17 April 2014 – Published: 3 June 2014

Abstract. The impact of future sea-level rise on coastal erosion as a result of a changing climate has been studied in detail over the past decade. The potential impact of a changing wave climate on erosion rates, however, is not typically considered. We explore the effect of changing wave climates on a pinned, soft-cliff, sandy coastline, using as an example the Holderness coast of East Yorkshire, UK.

The initial phase of the study concentrates on calibrating a numerical model to recently measured erosion rates for the Holderness coast using an ensemble of geomorphological and shoreface parameters under an observed offshore wave climate. In the main phase of the study, wave climate data are perturbed gradually to assess their impact on coastal morphology. Forward-modelled simulations constrain the nature of the morphological response of the coast to changes in wave climate over the next century. Results indicate that changes to erosion rates over the next century will be spatially and temporally heterogeneous, with a variability of up to ±25 % in the erosion rate relative to projections under constant wave climate. The heterogeneity results from the current coastal morphology and the sediment transport dynamics consequent on differing wave climate regimes.

1 Introduction

The coastal zone and immediate hinterland is a highly important socio-political domain (Pendleton, 2010). It is also amongst the most vulnerable, particularly when climate change alters sea level, weather systems and wave climates. Understanding the geomorphological response and sensitivity of coastal regions to these changes are key society-relevant scientific inquiries. Many studies have focussed on observation and monitoring, in order to understand the key processes and the rates at which they happen, particularly with regard to erosion or accretion along low-lying "soft" coasts dominated by weakly or unconsolidated sediments. Numerical modelling, parameterised in part by observational data, is increasingly used to study both coastal processes and the response of coastal evolution to climatic changes, under current conditions and those which might pertain in the future.

In this paper, we report a numerical modelling study of a soft-cliff, sandy coastline, which is pinned in place at the up-drift end by a rocky headland that resists erosion. We use the Holderness Coast, eastern England, as an example (Fig. 1). Whilst well studied and monitored (Scott Wilson, 2009; Quinn et al., 2009; Montreuil and Bullard, 2012), the possible future states of this coastline have received only minimal investigation using numerical modelling (Castedo et al., 2012). Efforts to understand this coastline are vital as it is among the most rapidly eroding of coastlines in Europe, with concomitant and serious threats to people, property, the local economy and infrastructure along its length. Valentin (1971) and de Boer (1964) showed that shoreline retreat at Holderness has been of the order of kilometres since the sea reclaimed the North Sea Basin at the end of the Quaternary. Many ancient settlements recorded in texts, such as the 12th century *Domesday Book* and old maps, have been lost to the sea. Current settlements and infrastructure con-

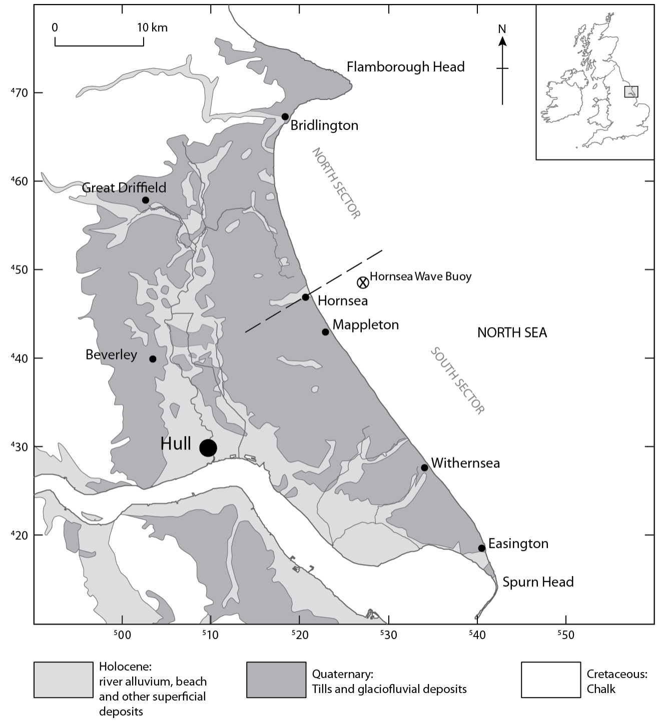

Figure 1. Geological composition of the Holderness coast (main) and the location of the region within the UK (insert). Also indicated are the positions of the Hornsea wave buoy, from which wave climate was recorded, and the division into northern and southern coastline regions, as referenced by the sea wall at Hornsea (dashed line), to aid analysis.

tinue to be lost, damaged or under imminent threat as the coastline retreats westwards. On the human level, loss of land and property can often be catastrophically rapid because of the episodic nature of cliff collapse over short timescales.

In order to understand the mechanisms and retreat rates within the Holderness littoral cell, and to develop a practical coastal management strategy (see Scott Wilson, 2009), most recent studies have focussed on monitoring and measurement of coastal position and beach profiles over several years (Quinn et al., 2009; Brown et al., 2012; Montreuil and Bullard, 2012). Modern observational techniques often use lidar scanning systems to provide accurate measurements of cliff retreat and volume loss. Many data sets of coastal change now exist to support coastal management decisions. However, such studies do not necessarily reflect what will happen in the future. The relatively short timescales over which these studies have been made inevitably represent only recent "snapshots" of geomorphological processes. Such geomorphological processes are stochastic, and therefore short records may not represent long-term-averaged conditions. These studies have limited predictive value, especially if the factors that control coastal evolution change significantly in the coming decades. Mesoscale modelling can allow long-term behavioural trends to be identified and explore the role of changes in driving forces. In addition, numerical modelling can be used to understand the morphological sensitivity of the Holderness coast under different climate change scenarios. Through modelling, the impact of such changes on settlements, land and infrastructure in the longer term can be assessed, even if only to show that current coastal recession, both in rate and form, is likely to continue in the forthcoming decades.

In order to investigate how a pinned, soft-cliff, sandy coastline might respond to future changes in hydrodynamic driving processes, and the rates at which such changes may occur, we have applied the numerical coastal evolution model, CEM (Ashton et al., 2001; Ashton and Murray, 2006a, b), to the Holderness coast. The model allows us to postulate how spatially and temporally sensitive the Holderness coastline is to differing wave climate scenarios. Changes to offshore wave height or approach angle modify gradients in alongshore transport, determining beach volume flux rates and subsequently cliff erosion rates. Previous work has shown that changing the distribution of wave-approach angles can change the shape of a sandy coastline (Slott et al., 2006; Moore et al., 2013); here we investigate how wave climate change scenarios affect the evolution of a soft-cliff coastline.

2 Geomorphology and wave climate of the Holderness coastline

2.1 Geomorphology

The Holderness coast stretches ~ 60 km from the chalk cliffs at Flamborough Head in the north to Spurn Head in the south (Scott Wilson, 2009; Quinn et al., 2009). The coastline is cut mainly in glacial till deposited during Devensian glaciations (c. 35 to 11.5 ka BP). Cliffs range from 2 to 35 m in height. The glacial till is composed of heterolithic clay, sand and gravel resting on a chalk platform sloping gently to the east (Catt, 2007). Coastal defences, including groynes, rock revetments and concrete sea walls, protect the larger towns and villages along the coastline. Recent recession rates, ranging between c. 1 m yr^{-1} and c. 5 m yr^{-1} depending on time and location, have been documented by Quinn et al. (2009) and Montreuil and Bullard (2012). South of Flamborough Head, wave-driven cliff erosion has created one of the fastest-retreating coastlines in Europe (IECS, 1994). With little external sediment transported into the Holderness coastline from the north (May, 1980), material derived from eroded cliffs supplies the bulk of the sediment flux southwards along the coastline. The Humber Estuary forms the southern boundary of the sediment cell, acting as a sink for sediment transported along the coast. The narrow sand and gravel spit at Spurn Head extends south-westwards across the mouth of the Humber for 3.5 km, and is known to have a complex, dynamically evolving morphology influenced by the inter-

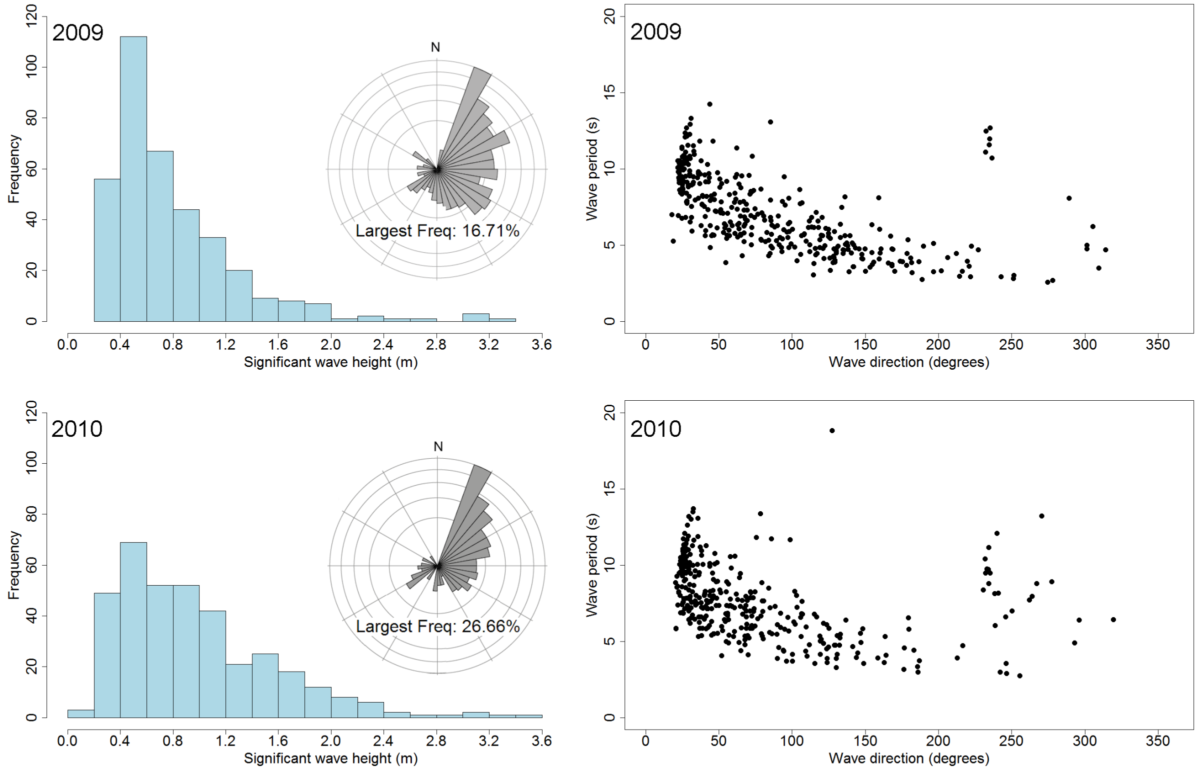

Figure 2. Wave climates used in the modelling. The data are daily averages, calculated from the data recorded every 30 min by the Hornsea WaveRider III buoy (CCO, 2013). The rose diagrams show the direction from which the wave is travelling. The "petals" are in 10° intervals and area-scaled by frequency percentage. The dominance of waves travelling from northeasterly directions is clear, particularly during 2010. Note the low frequencies of waves travelling in offshore directions. The histograms show that significant wave height data are positively skewed, but with marked variations in height frequencies over each year. Neither are well fitted to standard distributions, either in raw or transformed form. Overall, there were greater frequencies of higher waves in 2010, suggesting more unsettled weather than in 2009. $N = 365$ in both roses and histograms.

action of estuarine, tidal and longshore systems (Ciavola, 1997).

2.2 Recent historical wave climate

The current wave climate off the Holderness coast is recorded by the Hornsea Directional Waverider III buoy (CCO, 2013). This buoy has recorded mean half-hourly significant wave height, period and direction since June 2008. Wave climate is characterised by a north-easterly wave approach (Fig. 2), with a mean period of 7.3 s (2.6 to 18.8 s) and a seasonally variable significant wave height (0.2 to 3.5 m) with an annual mean of 0.9 m.

Daily averaged data for the years 2009 and 2010 are shown in Fig. 2; the term "historic" denotes this data set for the remainder of this manuscript. The dominant NNE mode exhibits frequency between 16 and 25 %. This mode was particularly strong in 2010. In 2009, modes from the ENE and ESE were more prominent. The differences in wave directions between the two years will be reflected in the modelled sediment fluxes and resultant coastal evolution. Significant wave heights were higher more frequently in 2010 than in 2009 (Fig. 2). The data show that seas off Holderness were rougher and more focussed in direction during 2010, and thus likely to cause more erosion and sediment transport than in 2009. A generally monotonic decline in wave period as the wave direction rotates clockwise from north (0°) can be observed in the buoy data (Fig. 2). The distribution of wave period with wave direction is similar for both 2009 and 2010, although the greater spread in wave direction is evident in the 2009 data. Wave periods lie within largely the same range in both years: between 4 and 14 s. On a few days, offshore waves, derived from the SW, have periods in the 8 to 14 s range. The longest period waves are mainly derived from the north-easterly direction, the dominant mode in wave direction. We infer these waves to be the long-period swell waves derived from North Atlantic low-pressure systems tracking across the north-eastern Atlantic, the waves refracting around northern Britain and down the North Sea. For just a few days each year, there are long-period waves travelling from a south-westerly direction.

2.3 Representing the future wave climate

Possible future wave climates for the North Sea have been studied in detail over the last decade, the motivation being to examine the effects of climate change on coastal flooding (Woth et al., 2006; Grabemann and Weisse, 2008) and ocean infrastructure (Wang et al., 2004).

Oceanic modes can increase or decrease the strength of incoming winds over Europe and have a dominant effect on the wave climate. For Europe, the North Atlantic Oscillation (NAO) is the dominant mode, modifying the path of the prevailing westerly winds and the position of storm tracks with a quasi-decadal frequency (Hurrell, 1995; Hurrell and van Loon, 1997). The NAO, and subsequently the intensity, frequency and tracks of storms, is likely to be affected by changes in climate over the coming century (Woollings et al., 2010). This is currently being studied using a multi-system modelling approach; greenhouse gas emission scenarios are used to force global circulation and regional climate models (IPCC, 2007), producing the atmospheric variables (wind speed and direction) needed in the derivation of wave climate using a wave model. The impact of future climate states on the NAO have not been quantified with any degree of certainty (Woollings, 2010); the triggering mechanisms for phase-switching, oceanic–atmospheric interactions that drive the system and teleconnections with other systems are poorly understood (Bladé et al., 2012).

Insufficient knowledge of the NAO combined with the range of greenhouse gas predictions and the variety of models used for research has produced a wide range of possible perturbations to future wind patterns and hence to future wave climates. Sutherland and Wolf (2002) linked a wave climate model to a coupled global climate model and found that predicted wave height changes are within ±5 % of current significant wave height. Due to the uncertainties inherent in the modelling, Hulme et al. (2002) provided a qualitative assessment of future wave climates in the Atlantic, suggesting modifications to the NAO would produce more westerly wave directions, therefore reducing wave height in the North Sea Basin. Further study by DEFRA (2010) on the impacts of climate change on wave climate highlights an increase in North Sea wave heights between 1973 and the mid-1990s, though more recent trends are unclear. Future UK wave climate projections were found to be very sensitive to the climate model scenarios for storms, which themselves are uncertain (DEFRA, 2010).

There are several ways to represent the future wave climate for the Holderness coast in the simulation phase of this study. Numerically simulated wave climate data could provide the required driving data; however, as discussed, there is a great deal of uncertainty currently associated with representing the large-scale systems which influence these data sets. With minimal re-engineering, observational wave climate data may be used to drive the future coastal modelling. Long-term observational data, which can be perturbed, exist for the North Sea Basin at several locations. However, the North Sea wave climate is non-linear and highly spatially heterogeneous, and it is therefore difficult to extrapolate non-local data to a specified location. Although only recorded over a 2-year period (at the time of the study), the historic recorded wave climate provides the best data set to drive model simulation, due to the locality of the observation point. For the calibration and baseline simulations (described in Sect. 4), these data are not perturbed. In the future scenarios, the offshore wave direction data are rotated by angles of between 0 and 20° in clockwise and anticlockwise directions, selected at random for each run. Similarly, significant wave heights are perturbed by up to ±0.4 m. To account for decadal to centennial-scale changes in wave climate, these adjustments to wave height and angle are applied linearly.

3 Modelling

Previous simulations of Holderness coastal morphology have focussed on cliff stability modelling at sub-centennial timescales. These studies employ two-dimensional cross-section models to consider rotational (e.g. Gibbons, 2004; Quinn et al., 2010) and translational (Robertson, 1990) cliff failure, with cliff topple as the prime coastal recession mechanism for the latter. Castedo et al. (2012) combine these failure mechanisms with the hydrodynamics and geotechnical characteristics of the coast determined at several locations, using observed recession rates to calibrate parameters. Future erosion rates at each location were calculated for the remainder of this century and found to have a quasi-linear response to sea-level rise. Potential changes in wave climate and their possible impact on the evolution of coastal morphology and retreat into the future have not been investigated. Two-dimensional planform models of coastal morphology allow the influence of wave climate variability on erosion and accretion rates along the coast to be explored. This section describes the model used in this study and its underlying conceptual framework.

We have adapted the coastline evolution model originally developed by Ashton et al. (2001), Ashton and Murray (2006a, b), and Valvo et al. (2006) to allow sediment inputs derived from cliff retreat (Fig. 3). Wave-generated erosion of a sea cliff may be spatially and temporally variable on short timescales (i.e. focused at the cliff toe, causing undercutting and subsequent overhang collapse; Young and Ashford, 2008); however at the decadal scale cliff retreat can be treated as a process considered to occur evenly over the entire cliff profile (Walkden and Hall, 2005; Limber and Murray, 2011, 2014; Limber et al., 2014). The rate of cliff retreat is thus time-averaged, and implicitly includes shorter-term changes such as storm-induced erosion (Sallenger et al.,

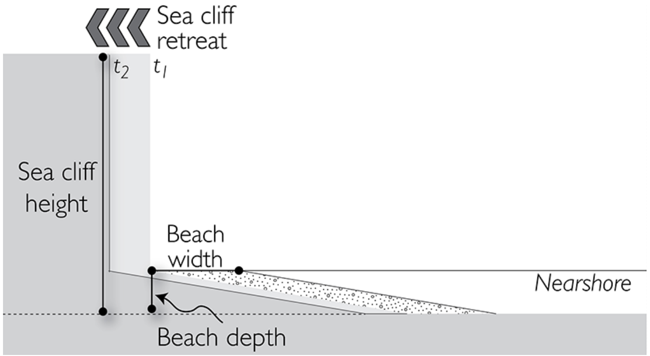

Figure 3. Cross-sectional view of the shoreface and cliff retreat variables, as defined for the modified coastal evolution model used in this study.

2002). For simplicity, model cliff topography is uniform, reflecting the mean cliff height of the Holderness coast.

Beach geometry and rates of sandy shoreline change are also averaged over short-term events (List et al., 2006). As the shoreline position changes, beach geometry remains constant, sediment is spread over the entire beach profile, and bathymetry contours are shore-parallel (Ashton and Murray, 2006a). The change in sandy coastline position (η_b) through time is governed by

$$\frac{\partial \eta_b}{\partial t} = -(1-\gamma HC)\frac{\mathrm{d}\eta_c}{\mathrm{d}t} + S - \left(\frac{1}{D}\frac{\partial Q_\mathrm{S}}{\partial x}\right), \tag{1}$$

where γ is a beach geometry constant that converts the volume of material eroded from the sea cliff into a beach width, H is sea-cliff height divided by the depth to which the beach extends, C is the proportion of sea-cliff material that is coarse enough to contribute to beach width (Limber et al., 2008), S is a beach sediment loss rate, D is the water depth (closure depth) to which shore-parallel bathymetry contours extend, Q_s is alongshore sediment transport (Ashton and Murray, 2006a); and x is alongshore position.

Equation (1) is discretised into uniform cells. The first term on the right-hand side represents sediment input into the coastal system as cliffs erode and rock is weathered into mobile sediment. There is an additional cliff retreat rate term (η_c) because the beach is pinned to the cliff as it retreats landward. The beach acts as a protective cover, reducing wave impact at the cliff toe. Accordingly cliff retreat rate is highest when local beach width (w) at a particular location is zero, decreasing exponentially as beach width increases (Sallenger et al., 2002; Valvo et al., 2006; Lee, 2008). To represent wave energy attenuation as waves refract towards the coastline (Adams et al., 2002), cliff retreat rate also depends on the mean daily breaking wave angle. The flux of coastal wave energy is maximised when waves approach a model cell orthogonally, and decreases as the incident wave angle increases. Cliff retreat through time is thus a function of wave angle and beach width calculated by

$$\frac{\mathrm{d}\eta_c}{\mathrm{d}t} = \cos(\varphi-\theta)\mathrm{Er}_0 e^{-\frac{w(t)}{w_\mathrm{scale}}}, \tag{2}$$

where φ is the incident angle of the deep-water wave; θ is the orientation of the coastline for a particular model cell; E_0 is the time-averaged, bare-rock cliff retreat rate; and w_scale is a length-scale constant dependent on beach width, which provides near-complete cover from wave attack, so that cliff retreat becomes negligible (i.e. $\sim 1\,\%$ of the maximum value; Sallenger et al., 2002; Limber and Murray, 2011). Different lithologies can be represented in the model by varying Er_0 and C: Er_0 represents erosional resistance, and C reflects the fraction of fine-grade sediment in the fallen material. More resistant lithologies (the chalk at Flamborough Head) have a lower Er_0 than rocks more susceptible to erosion (the glacial till along the Holderness embayment; Limber et al., 2014). Through a calibration process (described in Sect. 4), site-specific, uniform values for Er_0 and C can be set using long-term field observations of cliff retreat (e.g. Hapke and Reid, 2007). Although the model does not explicitly model the smaller-scale structural variations that affect the retreat rate of the rock, such as joints and fractures (Clark and Johnson, 1995; Trenhaile et al., 1998; Dickson et al., 2004), the long-term cliff retreat rate allows for implicit representation (e.g. structurally weaker rocks will have higher rates of retreat). This assumes a relatively even distribution of these features within a given rock type over a given spatial scale.

The second term in Eq. (1) represents constant beach sediment losses (S) through time due to, for example, the attrition and subsequent offshore transport of beach sediment in the surf zone, or as a human impact, such as sand mining (Thornton et al., 2006; Limber and Murray, 2011; Limber et al., 2014).

The final term represents the gradient in wave-driven alongshore sediment flux that causes large-scale, long-term shoreline change (erosion, accretion, the formation of capes and spits). Sediment flux is calculated via the common Coastal Engineering Research Center (CERC) sediment transport equation, as discussed at length elsewhere (Komar, 1971; Ashton et al., 2001; Ashton and Murray, 2006a, b; Valvo et al., 2006; List and Ashton, 2007; van den Berg et al., 2012). The magnitude of sediment flux is a function of incoming wave angle relative to the orientation of the coastline, and sediment transport occurs at a greater rate when wave height and period (through effects on shoaling and refraction) increase. Therefore, wave climate characteristics will have a marked effect on how sediment is distributed along a coastline and ultimately how large-scale coastal morphology will evolve.

A factor not expressed within Eq. (1) is the wave shadowing influence from protruding sections of coastline. The area covered by the shadowed zone is dependent on the incoming angle of the offshore wave, with respect to the shoreline, and the size of the headland. In the shadow, it is assumed that

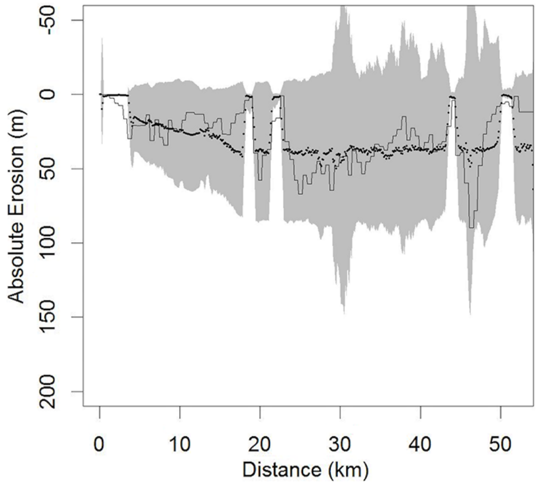

Figure 4. Range of simulated coastline retreat over a 15-year period, as captured during the ensemble calibration process (grey shadowing). The observed rates of change between 1995 and 2010 (modified from Montreuil and Bullard, 2012) are given as the solid black line and the ensemble member with the lowest RMSE plotted as a series of points for comparison.

there is no sediment transport when waves impinge beyond the critical angle at which shadowing occurs; however, sediment can be transported into this zone when waves approach at angles for which there is no shadowing (Ashton and Murray, 2006a).

In the original model, offshore wave climate is represented by a fixed offshore wave height and period, and by a four-bin probability density function (PDF), which defines the degree of asymmetry in wave direction and the fraction of high-angle waves (see Ashton et al., 2001). Recent wave climate records are available for the North Sea, off the coast of the Holderness cell, allowing a realistic representation of current wave climate (see Sect. 2). The model was therefore adapted to use observed wave records to drive the simulation. The major caveat in this conversion is that waves observed as propagating in an offshore direction, as determined by the average orientation of the coast, are converted to a null wave angle and height so that no sediment is transported during that time step.

4 Calibration and setup

The model is discretised into 100 m square cells, representing the region from Flamborough Head in the north to the Humber Estuary in the south, and a daily time step used to drive each simulation. The eastern boundary is approximately 40 km east of Hull and the western boundary 20 km to the west. The northern and southern boundaries of the model contain a mixture of nodes representing land, beach and sea, and use a specified boundary condition that allows a sand flux out of, but not into, the system. The western (land) and eastern (sea) boundaries are set with a no-flow condition such that sediment cannot be created, removed or passed through these interfaces. The Humber Estuary is represented as a sediment sink in the model. In reality, the Humber River transports sediment into the North Sea Basin, an area outside the model domain. For the purpose of this study we ignore the spit at Spurn Head, and this region is therefore excluded from both the calibration process and data analysis. The daily offshore wave height and angle, which provide energy for sediment transport in the model, are abstracted from the historic wave data, and cycled for the length of each simulation.

4.1 Calibration

Lithological and shoreface properties have been measured at several locations along the Holderness coastline (Newsham et al., 2002); however, these observations are spatially limited and are not likely to represent the coastline as a whole. To derive these parameters we ran the model 2000 times with different initial shoreface and lithological properties, and compare the simulated recession to observed rates using the root-mean-square error (RMSE). Observed recession rates used for this comparison are those compiled by Montreuil and Bullard (2012), spanning the 15-year period 1995–2010. To improve the RMSE between simulated and observed rates, larger coastal defences were represented in the simulation as slow-eroding surfaces. Each model run in the calibration is allocated 10 years of spin-up time, enough for each simulation to reach a steady-state condition, before the 15 years of simulation. Attenuation of steady state ensures that beach sediment, which is initialised as uniform along the coast, is distributed and that any small-scale roughness in the coastal profile used to initialise the coastline shape can be removed. The Monte Carlo (Metropolis and Ulam, 1949; Robert and Casella, 2004) approach adopted for the calibration process ensures that, for the main phase of simulation, the model is initialised with recession rates that are closest to those observed.

The closest simulated match to the observed recession data, and that selected to represent the lithological and shoreface parameters in the simulations used to project future coastal retreat, has an RMSE of 13.20 m and a mean error of 0.81 m (Fig. 4). The agreement between simulated and observed erosion rates is spatially variable along the coast. In the model we assume a homogeneous geology and topography and that the simulated coastline has a relatively uniform retreat rate around the designated coastal defences. Observational data show variable erosion along the coast and accelerated erosion down-drift of coastal defences. The difference in down-drift erosion around defences is due to the representation of wave refraction within the model (see Ashton and Murray, 2006a). The non-refraction differences are attributable to factors that may be considered either temporal or spatial. Temporally, the measured retreat rate reflects short-lived events such as storms and sand-bar placement, whereas the simulated retreat is averaged. Spatially, the susceptibility of the coastline to erosion is treated homogeneously in the model (apart from the division into hard and soft rock), whereas in reality, the geology is heterogeneous and many small-scale, engineered coastal defences are interspersed along the length of the coast. This heterogeneity is composed of regions more (due to joints and stream heads) and less (due to higher cohesion or hard coastal defences) susceptible to erosion. Erosional homogeneity is also affected by cliff failure and the subsequent protection this affords the new cliff face. These processes can be considered as implicit in the model if the process occurs evenly along the coast.

4.2 Future simulation

To assess the sensitivity of the coastline to possible future wave climates up to 2100, an ensemble of 1350 model runs is undertaken, with the historic offshore wave climate perturbed by up to $\pm 20°$ in rotation and up to ± 0.4 m significant wave height. These modifications to the historic wave climate, which is cycled at the end of each 2-year period, are applied linearly over the 90-year period from 2010 to 2100. Changes in offshore wave direction and significant wave height are selected at random between the bounding levels for each future simulation, with the initial state represented by the historic wave climate data. In addition to these perturbed future simulations, a baseline simulation is undertaken to gauge recession rates. This baseline simulation represents a future which continues to receive the same, unperturbed, historic wave climate and uses the same initialisation parameters as the future ensemble.

As we are assessing the response of a natural coastline to wave climate, the baseline and future ensemble simulations are undertaken without coastal defences. The rest of the model domain, grid-spacing and time-stepping attributes for these future simulations are identical to the calibration setup. To ensure the model is initialised from a steady state, a 10-year spin-up phase (as assessed during the calibration), starting from the current coastline position under current wave conditions, is performed before each simulation. The output from the spin-up period is omitted from the results and analysis. Erosion rates and sensitivity to wave climates are presented and discussed with reference to the start date 1 January 2010.

5 Results and analysis

Our analysis initially examines the spatial distribution of absolute erosion (recession) along the Holderness coast, and compares this recession relative to the baseline. By spatially averaging the relative erosion for each ensemble member, and plotting this value against the wave perturbation factors, the influences of rotating the wave climate and changing the wave height are examined. Finally, temporal analysis highlights the increasing diversity of the ensemble-relative erosion through the simulation period.

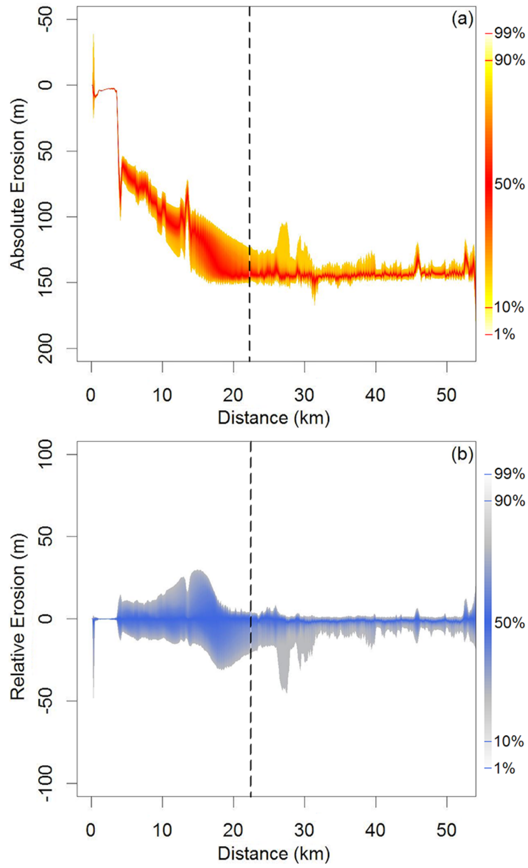

Figure 5. Simulated absolute change in coastline position **(a)** from 2010 to 2100 predicted using an ensemble of future wave climates. Relative change in coastline position **(b)**, as referenced to the baseline for each member of the ensemble. The range of colours in each plot represents the ensemble percentiles as given on the right of the figures. The black dashed line represents the divide between the northern region (to the left) and the southern region (to the right) as defined in the text.

5.1 Spatial analysis

The simulated distribution of absolute erosion along the coast by 2100, for the ensemble of wave climate perturbations, is presented in Fig. 5a. Zero erosion represents the initial coastline position for 2010, and positive values represent a landward coastal retreat. Landward retreat is near zero at Flamborough Head and increases to a maximum of 150 m in the central sections of the coastline. Toward the south, absolute erosion reduces in a quasi-linear fashion to 145 m at Easington (far right in the plot). Within this southern section of the coast, there is little range in the absolute erosion produced by the ensemble. The largest range in absolute erosion occurs at between 10 and 30 km south of the northern domain boundary, where the difference between the 10th and 90th percentiles is around 60 m.

When compared with the baseline (Fig. 5b) the results reveal that future erosion rates could either accelerate or slow depending on the nature of the wave climate change. The negative skewing of the relative erosion, where future simulations are compared to the baseline, implies that a reduction in erosion rate for the coast as a whole is more likely, although relative erosion along the coast is highly heterogeneous (Fig. 5b). The southern region (defined as south of the sea wall at Hornsea, Fig. 1) shows little variation in relative erosion, and the 50th percentile is close to zero. As with the absolute erosion rates, the northern region (defined as north and including the sea wall at Hornsea, Fig. 1) exhibits the greatest range in relative ensemble erosion rates over the 90-year period. The first to third quartiles also show a wide range of values in this region, indicating a spread of retreat values throughout the ensemble. Depending on the wave climate attributes of the ensemble member, there is up to ±30 m (∼ 25 %) disparity in erosion relative to the baseline.

5.2 Impacts of changing offshore wave angle and height

Spatially averaging relative change in erosion for each ensemble member allows an assessment of the individual and combined influences of rotating offshore wave direction and perturbing wave height.

Figure 6a shows that the relationship between changing offshore wave direction and relative erosion is linear within the range of −20 to 0°, with anticlockwise rotation progressively reducing relative erosion. Clockwise rotation in the offshore wave climate of up to 18° increases erosion rates, although unlike the anticlockwise trend, this trend is nonlinear. There is further asymmetry between clockwise and anticlockwise offshore wave rotations where, under certain circumstances, clockwise rotation greater than 18° reduces recession in comparison to the baseline.

The influence of a changing wave height on relative erosion is presented in Fig. 6b. It reveals a weak relationship, where a reduction in relative erosion occurs with increasing wave height. Mean relative erosion ranges between −8 and 5 m under a wave height reduction of 0.4 m, and between −13 and 4 m under a wave height increase of 0.4 m.

The range in relative erosion for a particular offshore wave height or rotation is partially controlled by the corresponding perturbation. For example, the range of relative erosion determined for a fixed offshore wave rotation of −10° is a function of the range of wave heights. This suggests that both wave parameters influence relative erosion, although the strongest control remains offshore wave rotation, as this generates the smallest range in relative erosional for any fixed rotation value. To highlight the relationship between relative erosion and perturbations in offshore wave height and rotation, they are plotted together in Fig. 6c and d. As highlighted in previous plots, a clockwise rotation results in increased relative erosion and an anticlockwise rotation less relative erosion. The small, subtle effects of changing wave height are also highlighted: for any particular offshore wave rotation, the relative erosion rate decreases by a small amount as wave height increases. These relationships alter under the most extreme clockwise changes (under offshore wave rotations above 18°), where greater wave heights increase relative erosion.

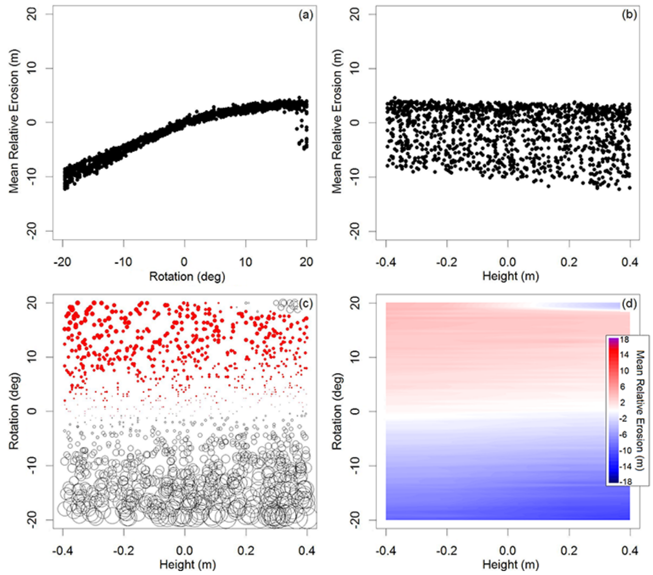

Figure 6. Wave rotation **(a)** and wave height **(b)** components of wave climate plotted against spatially averaged mean relative erosion over the 90-year period. Negative erosion values indicate a relative reduction in the erosion rate in comparison to the baseline. Wave height and rotation perturbation factors are plotted together **(c)**. The size of each symbol is relative to the change in mean erosion rate imparted by that wave climate in comparison to the baseline scenario. Red dots represent increased erosion relative to the baseline and empty circles reduced erosion. The same data have been a contoured **(d)**. The scale on this plot represents spatially averaged (mean value for the coast as a whole) relative erosion (m) after 90 years of simulation.

5.3 North–south divide

The northern and southern regions of the coastline respond differently to changes in wave climate. To assess these differences, the relative change in erosion for each region is presented in spatially averaged forms (Figs. 7 and 8).

In the northern region, there is a highly linear coupling between offshore wave rotation and erosion, even under clockwise rotations. The reduction in relative erosion, apparent at the extreme of clockwise rotation for some ensemble members, where the whole coastline is considered (see Fig. 6), is not apparent in the northern region. For this region there is no definitive relationship between changing wave height and relative erosion.

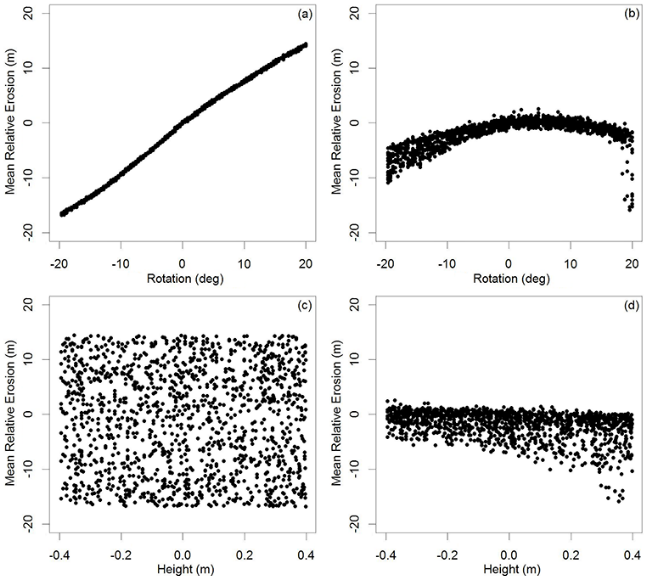

Figure 7. Wave rotation perturbation plotted against spatially averaged mean relative erosion for the north **(a)** and south **(b)**. Negative values indicate a reduction in the erosion rate. Wave height perturbations are also plotted against spatially averaged mean relative erosion for the north **(c)** and south **(d)**.

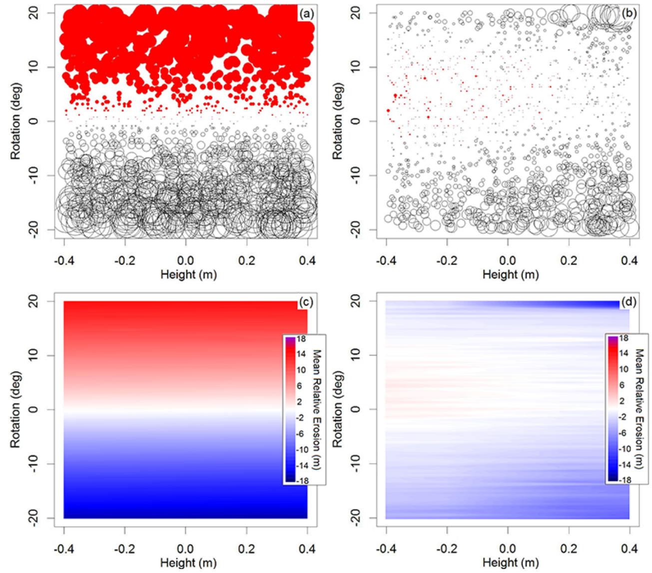

Figure 8. Wave height and rotation perturbation factors are plotted against each other for the north **(a)** and south **(b)** of the model domain. The size of each symbol is relative to the change in mean erosion rate imparted by that wave climate in comparison to the baseline scenario. Red dots represent increased erosion relative to the baseline and empty circles reduced erosion. Interpolated contour plots of the height change component of wave climate against the wave rotation component for the north **(c)** and south **(d)** of the model domain are also given.

In the south, maximum relative erosion occurs at clockwise rotations of around 8°. In comparison to the north, the range of relative erosion is lower in the south, suggesting a balance in the height and rotation perturbations. The relationship between increasing wave height and relative erosion reduction is broadly linear in the south. This relationship produces a weak gradient under small rotations in offshore wave climate, but with large clockwise rotations the gradient in increased. This trait is highlighted in Fig. 8, where, for the southern region, there is a relatively strong horizontal gradient in relative erosion at clockwise offshore wave rotations above 18°.

5.4 Temporal evolution

By plotting the average relative erosion against time, arising temporal divergences were elucidated (Fig. 9). Throughout the simulation, the average relative erosion rate remains near zero. Over the first 40 years of simulation, the range of possible erosion rates show little asymmetry, indicating a low tendency for either increased or decreased erosion rates. Modifications to the wave climate over this period are small, as the wave climate perturbations are applied linearly to the baseline climate for each scenario. As the wave factors begin to impart a larger influence, there is a non-linear response from the system. The range between both the outliers and the first and third quartiles get progressively larger. The data become negatively skewed, implying that a reduction in relative erosion is more likely given the input parameters of the ensemble.

6 Discussio

The following discussion highlights three overarching impacts of morphology on recession that may be extrapolated to similar coastlines. Detail is provided for the Holderness coast; however, separate analysis would be required to determine the same level of detail for a different coastline of similar morphology.

Overall, the response of the Holderness coastline to modified wave climates is a reduction in relative recession. This reduction is due to a tendency for the future wave climates to move the average offshore wave angle (with respect to coastline orientation) away from the sediment transport peak of 42° as defined in the underlying CERC equation. The coastline response is spatially heterogeneous, with different sections of the coastline exhibiting variable rates of erosion under differing wave climate scenarios. In the north, clockwise offshore wave climate rotations increase relative erosion and anticlockwise rotations reduce erosion. In the south, increased relative erosion peaks occur at a clockwise wave climate rotation of about 5°. The difference in recession rates for the northern and southern sections of the model is due to a combination of factors. Firstly, the angle between that of

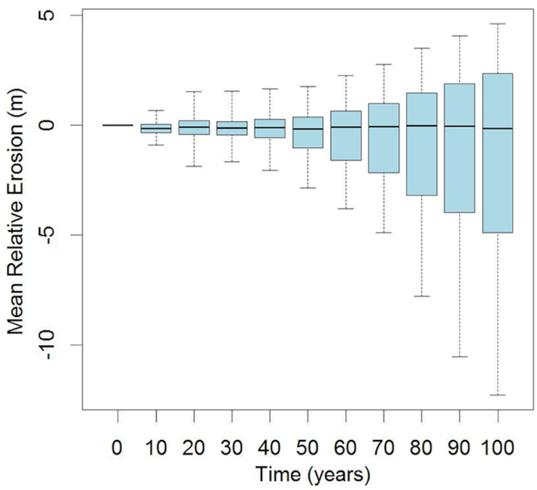

Figure 9. Box-and-whisker plot showing the evolution of spatially averaged mean relative coastal erosion, in comparison to the baseline, through time. The central bars represent the median value, the blue boxes show the interquartile range and the extended bars represent extreme values.

the wave direction and the coast increases towards the south as the coastline orientation changes. Secondly, there is a heterogeneous distribution of beach sediment through time and space, and hence variable protection from erosion, along the coast. Thirdly, the CEM accounts for shadowing of the coast by headlands, and thus Flamborough Head shadows the north and protects this region from erosion under certain wave climates. Here we discuss the relative importance of these three factors in driving the heterogeneous erosion rates.

6.1 Shoreline angle

Neglecting wave-shadowing effects (considered below), alongshore changes in coastline orientation tend to cause shoreline change. The dominant observed offshore wave direction in the historic data set is approximately 30°. This results in angles with the coastline of between 20 and 90° in the north region and an approximately constant 20° in the south. The variation in coastline orientation with respect to the incoming wave direction tends to create a gradient in transport, and associated shoreline change, that is strong in the north.

Changes in offshore wave-approach angles will tend to affect part of the northern section especially strongly. Modelled sediment transport is greatest when offshore waves impinge the coast at relative angles of between 30 and 50°, depending on the equation used for breaking-wave-driven, alongshore sediment transport (Ashton and Murray, 2006a). For the CERC equation, as used by the CEM, maximum sediment transport occurs at 42°. Parts of the coastline within the northern region are orientated close to this angle, with respect to the dominant offshore wave direction. Changes in relative wave-approach angles generally cause a shift in coastline diffusivity; the rate that shoreline curvature is smoothed out, or the rate that it is exaggerated in the case where waves approach from angles greater than the one that maximises alongshore sediment flux (Ashton et al., 2001). In the relationship between coastline diffusivity and relative wave angle, the gradient (slope of the curve) is greatest for the wave-approach angle that maximises alongshore sediment flux (Ashton and Murray, 2006a). For those parts of the coastline with orientations close to the one that maximises the net alongshore flux for a given distribution of wave-approach angles, changes in the dominant wave-approach direction will tend to have the greatest effect in changing coastline diffusivity, and therefore shoreline change rates. For some coastline segments, changing diffusivity could even involve a shift from a tendency toward diffusive coastline dynamics (accretion in concave-seaward segments) to anti-diffusion (erosion where the coastline is concave), and vice versa. These coastline-curvature effects partially explain the spatial variation in the relative sensitivity of the north and south coastal sections to changes in wave direction.

6.2 Sand protection and the impact of increasing wave height

The spatial variation in erosion contributes to the morphological sensitivity of the Holderness coastline, as the majority of transported sediment is derived from the cliffs within the coastal domain. In the simulation, beach volume is spatially heterogeneous at any particular time, tending to reflect pulsed fluxes of sediment migrating in the southerly longshore drift direction. These flux pulses are relatively small in the north, where sediment input is limited. They increase in size towards the centre of the model, where they reach a maximum, migrating at around 1 km yr^{-1}. Although differing in shape, these pulses are analogous to the "ord" sandbars described and discussed by Pringle (1985). The ords are formed in the northern part of the coast, where the shadowing effect of Flamborough Head begins to diminish. Their formation in the northern region of the model is controlled by the driving wave climate. The influence of high-angle waves (those approaching from angles greater than the alongshore-flux-maximising angle) in the northern section favours the development of simulated ords (Ashton and Murray, 2006a).

As described by Pringle (1985), ords and their migration affect coastal erosion. Where the ords cover and protect the shoreface and cliff base, erosion rates are reduced, while they are enhanced between the ords where the protection is reduced. The movement of these sand bodies along the shoreface, integrated over the decadal to centennial scale, reduces erosion rates along the entire coast, relative to a situation in which protective sand cover is absent. However, because of the concave-upward (exponential) relationship between beach width and cliff erosion rate in the model, the formation of ords in the model could also enhance long-term erosion rates relative to a smoother alongshore distribution of protective sediment. A thought experiment helps to explain this effect. Starting with an alongshore-uniform distribution of a given amount of sediment, rearranging that sediment into pulses tends to reduce cliff erosion rates where beach width is increased. This tends to reduce alongshore- or time-averaged cliff erosion rates. However, because of the concavity of the beach-width cliff-erosion-rate curve, compared to the decreased cliff erosion, where beach widths are increased, cliff erosion is increased more where widths are decreased. Therefore, the effect of increasing the heterogeneity of beach widths (whilst fixing the amount of sediment along a coastline segment) is to enhance averaged cliff erosion rates. For a coastline section in which part of the coast is bare of sediment, so that cliff-erosion rates locally (and temporarily) dictate shoreline change rates, the migration of ords could increase long-term erosion.

The relationship between protective beach cover and cliff erosion rates could explain the effect that changing wave height has on erosion rates. One possible explanation for this wave-height effect involves cliff erosion rates in the northernmost section of the coastline. As there is no influx of sediment around Flamborough Head, beach widths in the most northerly regions cannot grow sufficiently to protect the soft-till cliffs from erosion. Increasing wave height laterally extends this zone of reduced beach protection by increasing the gradient in sediment transport, generating more sediment input from cliff retreat and increasing the availability of sand for beach protection further south. The reduction in erosion created by the added beach protection outweighs the increased erosion along the cliffs in the north, reducing overall erosion along the coast when wave height is increased.

Another possibility (not mutually exclusive with the first one), involves the relationship between wave heights and the diffusivity of the wave climate. Holding the distribution of wave-approach angles fixed, increasing offshore wave height tends to increase coastline diffusivity (Ashton and Murray, 2006a). In the southerly parts of the domain, where the ords migrate along the coastline, increasing coastline diffusivity would tend to smooth out the ords, making them less pronounced (Ashton and Murray, 2006a). This tendency to reduce alongshore variability in beach width reduces the long-term shoreline erosion rate if the coastline is intermittently bare; as ords migrate through the domain making erosion rates intermittently limited by detachment rate (as opposed to transport limited). Determining the dominant cause for the wave-height effect on coastline erosion rates will require additional analysis of model results beyond this study.

6.3 Shadow zone

The final effect on variations in simulated erosion involves the shadow zone caused by Flamborough Head. As the shoreline extends seawards to a headland (Flamborough Head), portions of the shoreline are shadowed to waves of particular orientations. At each time step in the model, the wave direction is determined and the shoreline scanned for shore segments that are shadowed. Wave height, and concurrently sediment transport, within the shadow is set to zero. This method assumes the headland is a prominent coastal feature and therefore that wave energy retained for sediment transport following refraction is greatly reduced. Ashton and Murray (2006a) provide a detailed description of the shadow function with the CEM. The extent of the shadowed region changes with changing offshore wave direction at each time step. Within any stretch of coastline that is shadowed part of the time, moving down-drift from the headland, the degree of shadowing decreases, which tends to produce a divergence of alongshore sediment flux and associated erosion. Within a shadow zone, large-scale concave-seaward coastline curvature tends to develop from this shadow-related erosion, as the alongshore gradients in shoreline orientation tend to adjust, producing alongshore-uniform erosion rates (which are determined by the boundary conditions).

In our study area, due to the orientation of Flamborough Head, waves from the north create the largest shadow zone, while waves from the east and south produce no shadow zone. With an increasingly rotating offshore wave climate, the area shadowed by the headland is progressively modified and the sediment transport rates along the coastline changed accordingly. Anticlockwise rotations will increase shadowing in the northern section, which reduces net alongshore sediment fluxes, and therefore the potential for erosion. Conversely, clockwise rotation will reduce the shadowing and increase the potential for erosion. Perhaps most importantly, changing the portion of the waves from which the coastline is shadowed changes local wave climates along that coastline, and due to the shape of the coastline, the impacts of these changes are asymmetrical with respect to the direction of wave climate rotation. Anticlockwise rotation will remove more of the high-angle waves felt by coastline segments within the northern section. This loss of high-angle influence will tend to make the local wave climates more diffusive, favouring more sediment retention in the concave-seaward northern coastline section. Clockwise rotations, on the other hand, tend to make the local wave climate less diffusive, favouring an increase in the coastline curvature through erosion in the central northern section.

7 Caveats

Although the model produces a reasonable representation of erosion rates during calibration, it is important to highlight the caveats of using such a model for sensitivity analysis. The basis for many of these caveats surrounds the simplified representation of physical processes within the CEM.

The geology within each erodible rock type for the simulation is assumed to be homogeneous and free from any dominating, anisotropic features, such as rivers or major fractures. Smaller-scale features are integrated implicitly in the lithological and shoreface properties determined by the calibration phase. However, larger features, such as the stream mouth north of Withernsea, will not be properly reflected by the model. In addition to these natural heterogeneities, it is recognised that negation of coastal defence structures within the simulation will alter the evolving morphological characteristics of the represented coast. These defences act as non-erodible surfaces, arresting the landward retreat of the coastline. These features are intentionally ignored as we are assessing the natural morphological sensitivity of the coast.

The single division of rock susceptibility to erosion within the model allows Flamborough Head to remain a prominent headland. The complete geometric shadowing assumed by the model on the down-drift side of a headland forms a region in the model with no sediment transport processes. In reality, complex refraction, and diffraction, of the wave around the headland would occur, sending a part of the wave energy into the shadowed zone and modifying the approach angle of waves. However, the main effect of greatly reducing sediment transport within the shadow is captured.

The remaining caveats are concerned with the representation of the future state of the North Sea within the model. A future wave climate is unlikely to be similar to the simply perturbed historic wave climate used in this study. It assumes that weather patterns are essentially the same as they were in 2009–2010, and there has been no attempt to reflect possible changes in storminess. However, by using an ensemble approach, the range of likely effects on the morphological characters of the Holderness coastline is captured.

Finally, predicted sea-level rise for the Holderness coast should not have a significant influence on wave climate, and the direct influence on coastal recession is thought to be quasi-linear. Thus, the simulation undertaken here does not include sea-level rise and our results need to be considered in conjunction with estimates of recession rates from such rises. Bray and Hooke (1997) suggested an increase in recession rates of between 22 and 133 % by 2050 using a modified Bruun rule method, while Castedo et al. (2012) used their cliff recession model to derive a linear increase in recession rates ranging from 0.015 m yr^{-1} for an annual sea-level increases in of 1 mm to 0.32 m yr^{-1} for an annual sea-level increase of 10 mm.

8 Conclusions

An ensemble of 1350 simulations of coastal erosion is undertaken, each forced with a gradually perturbed version of a recorded, historic wave climate to represent the period from 2010 to 2100. A baseline run is undertaken using the historic wave climate from 2009 to 2010, cycled over 90-years. This provides a reference against which to compare the output from the simulations using the stochastically varied wave climate.

Considering the Holderness coast as a whole, anticlockwise rotation of the wave climate broadly reduces the rate of erosion, whilst clockwise rotations increase rates. Although the correlation is less strong, wave heights also have an impact on erosion; however, due to changes in sediment distribution, they unexpectedly lead to an average reduction in relative erosion with increasing height. The sensitivity of the coast to these changes in offshore wave climate is spatially variable, with broadly differing impacts in the northern and southern regions.

Fundamental changes to the system due to the changing offshore wave climate do not occur in the first 40 years of simulation. In the following years to 2100, landward retreat remains close to zero for the chalk outcrop in the north, which pins the system. The combination of incident wave angle, wave shadowing and variable beach protection results in northern regions of the coast exhibiting the greatest sensitivity to changes in wave climate. Difference in the relative influences of perturbations in offshore wave height and rotations of wave direction are found for the northern and southern regions of the Holderness coast. These differences suggest that erosion in the northern region is more sensitive to changes in offshore wave direction, while erosion in the southern region is sensitive to combined changes in wave height and wave direction.

Acknowledgements. The authors are grateful to Martin Hurst of the British Geological Survey for reviewing this paper and returning feedback that led to its improvement. This paper is published with the permission of the Executive Director of the British Geological Survey (NERC), and was supported by the Climate and Landscape research programme at the BGS.

Edited by: S. Mudd

References

Adams, P. N., Anderson, R. S., and Revenaugh J: Microseismic measurement of wave energy delivery to a rocky coast, Geology, 30, 895–898, 2002.

Ashton, A. and Murray, A. B.: High-angle wave instability and emergent shoreline shapes: 1. Modeling of sand waves, flying spits, and capes, J. Geophys. Res. Earth Surf., 111, F04011, doi:10.1029/2005JF000422, 2006a.

Ashton, A. and Murray, A. B.: High-angle wave instability and emergent shoreline shapes: 2. Wave climate analysis and comparisons to nature, J. Geophys. Res. Earth Surf., 111, F04012, doi:10.1029/2005JF000423, 2006b.

Ashton, A., Murray, A. B., and Arnoult O: Formation of coastline features by large-scale instabilities induced by high-angle waves, Nature, 414, 296–300, 2001.

Bladé, I., Liebmann, B., Fortuny, D., and van Oldenborgh, G. J.: Observed and simulated impacts of the summer NAO in Europe: implications for projected drying in the Mediterranean region, Clim. Dynam., 39, 709–727, 2012.

Bray, M. J. and Hooke, J. M.: Prediction of soft-cliff retreat with accelerating sea-level Rise, J.Coastal Res., 13, 453–467, 1997.

Brown, S., Barton, M. E., and Nicholls, R. J.: The effect of coastal defences on cliff top retreat along the Holderness coastline, P. Yorks. Geol. Soc., 59, 1–13, 2012.

Castedo, R., Murphy, W., Lawrence, J., and Paredes, C.: A new process–response coastal recession model of soft rock cliffs, Geomorphology, 177/178, 128–143, 2012.

Catt, J. A.: The Pleistocene glaciation of eastern Yorkshire: a review, P. Yorks. Geol. Soc., 56, 177–207, 2007.

CCO: Channel Coastal Observatory, http://www.channelcoast.org/data_management/real_time_data/charts/?chart=72, las access: July 2013, 2013.

Ciavola, P.: Coastal dynamics and impact of coastal protection works on the Spurn Head spit (UK), Catena, 30, 369–389, 1997.

Clark, H. C. and Johnson M. E.: Coastal Geomorphology of Andesite from the Cretaceous Alisitos Formation in Baja California (Mexico), J. Coastal Res., 11, 401–414, 1995.

de Boer, G.: Spurn Head: its history and evolution, T. I. Brit. Geogr., 34, 71–89, 1964.

DEFRA: Charting Progress 2. Feeder Report: Ocean Processes, Department for Environment Food and Rural Affairs, on behalf of the UK Marine Monitoring and Assessment Strategy community, Department for Environment Food and Rural Affairs on behalf of the UK Marine Monitoring and Assessment Strategy community, Nobel House, London, UK, 2010.

Dickson, M. E., Kennedy, D. M., and Woodroffe, C. D.: The influence of rock resistance on coastal morphology around Lord Howe Island, southwest Pacific, Earth Surf. Proc. Land., 29, 629–643, 2004.

Gibbons, C. R.: A study of the different types of landslides and the associated rates of recession along the Holderness coast, East Yorkshire, MSc thesis, University of Leeds, 2004.

Grabemann, I. and Weisse, R.: Climate change impact on extreme wave conditions in the North Sea: an ensemble study, Ocean Dynam., 58, 199–212, 2008.

Hapke, C. and Reid, D.: National assessment of shoreline change, Part 4: Historical coastal cliff retreat along the California coast, US Geological Survey Open-file Report, 2007–1133, 1–51, 2007.

Hulme, M., Jenkins, G., Lu, X., Turnpenny, J., Mitchell, T., Jones, R., Lowe, J., Murphy, J., Hassell, D., Boorman, P., Macdonald, R., and Hill, S.: Climate-Change Scenarios for the United Kingdom: The UKCIP02 Scientific Report, Tyndall Centre for Climate Change Research, 2002.

Hurrell, J. W.: Decadal trends in the North-Atlantic Oscillation – Regional temperatures and precipitation, Science, 292, 676–679, 1995.

Hurrell, J. W. and van Loon, H.: Decadal variations in climate associated with the North Atlantic Oscillation, Clim. Change, 36, 301–326, 1997.

IECS: Humber Estuary and Coast, Institute of Estuarine and Coastal Studies, University of Hull, Hull, UK, 1994.

IPCC: Climate Change 2007: vol 4, Cambridge University Press, Cambridge, UK, 2007.

Komar, P. D.: The mechanics of sand transport on beaches, J. Geophys. Res., 76, 713–721, 1971.

Lee, E. M.: Coastal cliff behaviour: Observations on the relationship between beach levels and recession rates, Geomorphology, 101, 558–571, 2008.

Limber, P. W. and Murray, A. B.: Beach and sea cliff dynamics as a driver of rocky coastline evolution and stability, Geology, 39, 1149–1152, 2011.

Limber, P. W. and Murray, A. B.: Unraveling the dynamics that scale cross-shore headland relief on rocky coastlines, Part 2: Model predictions and initial tests, J. Geophys. Res. Earth Surf., doi:10.1002/2013JF002978, in press, 2014.

Limber, P. W., Patsch, K. B., and Griggs G. B.: Coastal sediment budgets and the littoral cut-off diameter: A grain-size threshold for quantifying active sediment inputs, J. Coastal Res., 24 (supplement 2), 122–133, 2008.

Limber, P. W., Murray, A. B., Adams, P. N., and Goldstein, E. B.: Unraveling the dynamics that scale cross-shore headland relief on rocky coastlines, Part 1: Model development, J. Geophys. Res. Earth Surf., doi:10.1002/2013JF002950, in press, 2014.

List, J., Farris, A. H., and Sullivan, C.: Reversing storm hotspots on sandy beaches: spatial and temporal characteristics, Mar. Geol., 226, 261–279, 2006.

List, J. H. and Ashton, A. D.: A circulation modeling approach for evaluating the conditions for shoreline instabilities, Coastal Sediments 2007, Am. Soc. of Civ. Eng., Reston, Va, 327–340, 2007.

May, V. J.: Flamborough Head, Volume 28: Coastal Geomorphology of Great Britain Chapter 4: Soft-rock cliffs - GCR site reports, J. S. Publications, Suffolk, UK, 1980.

Metropolis, N. and Ulam, S.: The Monte Carlo method, J. Am. Statist. Assoc., 44, 335–341, 1949.

Montreuil, A.-L. and Bullard, J. E.: A 150-year record of coastline dynamics within a sediment cell: Eastern England, Geomorphology, 179, 168–185, 2012.

Moore, L. J., McNamara, D. E., Brenner, O., and Murray, A.B., 2013. Observed changes in hurricane-driven waves explain the dynamics of modern cuspate shorelines, Geophys. Research Lett., 40, 5867–5871, doi:10.1002/2013GL057311, 2013.

Newsham, R., Balson, P. S., Tragheim, D. G., and Denniss, A. M.: Determination and prediction of sediment fields from recession of the Holderness Coast, NE England, J. Coastal Conserv., 8, 49–54, 2002.

Pendleton, L. H.: The economic and market value of coasts and estuaries: what's at stake?, Coastal Ocean Values Press, Washington, DC, USA, 2010.

Pringle, A. W.: Holderness coast erosion and the significance of ords, Earth Surf. Proc. Land., 10, 107–124, 1985.

Quinn, J. D., Philip, L. K., and Murphy, W.: Understanding the recession of the Holderness Coast east Yorkshire, UK: a new presentation of temporal and spatial patterns, Q. J. Eng. Geol. Hydroge., 42, 165–178, 2009.

Quinn, J. D., Rosser, N. J., Murphy, W., and Lawrence, J. A.: Identifying the behavioural characteristics of clay cliffs using intensive monitoring and geotechnical numerical modelling, Geomorphology, 120, 107–122, 2010.

Robert, C. P. and Casella, G.: Monte Carlo Statistical Methods. Secaucus, NJ, USA: Springer, New York, Inc., 2 Edn., 2004.

Robertson, I.: Erosion and Stability of Till Cliffs on the Holderness Coast, Ph.D. Thesis, University of Newcastle Upon Tyne, University of Newcastle Upon Tyne, Newcastle, UK, 1990.

Sallenger, A. H., Krabill, W., Brock, J., Swift, R., Manizade, S., and Stockdon, H.: Seacliff erosion as a function of beach changes and extreme wave runup during the 1997–1998 El Nino, Mar. Geol., 187, 279–297, 2002.

Scott, W.: Humber Estuary Coastal Authorities Group (HECAG), Flamborough Head to Gibraltar Point Shoreline Management Plan 2, Scott Wilson, Basingstoke, Hampshire, UK, 2009.

Slott, J. M., Murray, A. B., Ashton, A. D., and Crowley, T. J.: Coastline responces to changing storm patterns, Geophys. Res. Lett., 33, L18404, doi:10.1029/2006GL027445, 2016.

Sutherland, J. S. and Wolf, J.: Coastal defence vulnerability 2075, HR Wallingford Report SR590, H R Wallingford, Wallingford, UK, 2002.

Thornton, E. B., Sallenger, A., Conforto, S. J., Egley, L., McGee, T., and Parsons, R.: Sand mining impacts on long-term dune erosion in southern Monterey Bay, Mar. Geol., 229, 45–58, 2006.

Trenhaile, A. S., Pepper, D. A., Trenhaile, R. W., and Dalimonte, M.: Stacks and notches at Hopewell Rocks, New Brunswick, Canada, Earth Surf. Proc. Land., 23, 975–988, 1998.

Valentin, H.: Land Loss at Holderness, Applied Coastal Geomorphology, edited by: Steers, J. A., 1 Macmillan, 16–137, 1971.

Valvo, L., Murray, A. B., and Ashton, A.: How does underlying geology affect coastline change? An initial modeling investigation, J. Geophys Res. Earth Surf., 111, F02025, doi:10.1029/2005JF000340, 2006.

van den Berg, N., Falqués, A., and Ribas, F.: Modeling large scale shoreline sand waves under oblique wave incidence, J.Geophys Res. Earth Surf., 117, F03019, doi:10.1029/2011JF002177, 2012.

Walkden, M. J. A. and Hall, J. W.: A predictive mesoscale model of the erosion and profile development of soft rock shores, Coast. Eng., 52, 535–563, 2005.

Wang, X. L., Zwiers, F. W., and Swail, V. R.: North Atlantic Ocean Wave Climate Change Scenarios for the Twenty-First Century, J. Climate, 17, 2368–2383, 2004.

Woollings, T.: Dynamical influences on European climate: an uncertain future, Phil. Trans. R. Soc. A, 368, 3733–3756, 2010.

Woollings, T., Hannachi, A., Hoskins, B., and Turner, A.: A Regime View of the North Atlantic Oscillation and Its Response to Anthropogenic Forcing, J. Climate, 23, 1291–1307, 2010.

Woth, K., Weisse, R., and von Storch, H.: Climate change and North Sea storm surge extremes: an ensemble study of storm surge extremes expected in a changed climate projected by four different regional climate models, Climate Dynam., 26, 3–15, 2006.

Young, A. P. and Ashford, S. A.: Instability investigation of cantilevered seacliffs, Earth Surf. Proc. Land., 33, 1661–1677, 2008.